Eidgenössische Technische Hochschule Zürich

Ecole polytechnique fédérale de Zurich
Politecnico federale di Zurigo
Swiss Federal Institute of Technology Zurich

Multidimensional High Order Method of Transport for the Shallow Water Equations.[1]

A.-T. Morel, M. Fey and J. Maurer

Research Report No. 96-09
July 1996

Seminar für Angewandte Mathematik
Eidgenössische Technische Hochschule
CH-8092 Zürich
Switzerland

[1]To appear in "Proceeding of the ECCOMAS 96 Conference", Paris, Sept. 9-13, 1996.

Multidimensional High Order Method of Transport for the Shallow Water Equations.[1]

A.-T. Morel, M. Fey and J. Maurer

Seminar für Angewandte Mathematik
Eidgenössische Technische Hochschule
CH-8092 Zürich
Switzerland

Research Report No. 96-09 July 1996

Abstract

The Method of Transport was originally developed for the Euler equation in 1993 by M. Fey. He introduced the physical property of infinitely many propagation directions into the numerical method. Here, we present the extension of this method to equations with inhomogeneous fluxes, such as the shallow water equations. For efficiency reasons and to reach higher order accuracy certain modifications had to be made to the method, whereby the multidimensional character will be kept. The resulting scheme can then be interpreted as a decomposition of the nonlinear equations into a system of linear advection equations with variable coefficients in conservative form. We present a multidimensional high order resolution scheme for the advection equation and for the shallow water equations. A special limiting technique is used for these methods to keep the multidimensional properties.

Keywords: Shallow water equations, multidimensional schemes, method of transport, second order, correction terms.

Subject Classification: AMS(MOS) subject classifications (1991): 65M06, 65M25, 35L65, 35L70, 76M25.

[1] To appear in "Proceeding of the ECCOMAS 96 Conference", Paris, Sept. 9-13, 1996.

1. Introduction

The two-dimensional shallow water equations in conservation form read

$$\underline{U}_t + \nabla \cdot \underline{\underline{\mathcal{F}}} = 0, \tag{1}$$

with

$$\underline{U} = \begin{pmatrix} h \\ h\,\underline{u} \end{pmatrix}$$

the state vector, where h is the total depth of the fluid and $\underline{u} = (u, v)^T$ the velocity vector. The divergence acts on the rows of the flux matrix $\underline{\underline{\mathcal{F}}}$ given by

$$\underline{\underline{\mathcal{F}}} = \underline{U}\,\underline{u}^T + \frac{h\,c^2}{2}\begin{pmatrix} \underline{0}^T \\ \underline{\underline{I}} \end{pmatrix},$$

where $c = \sqrt{g\,h}$ is the celerity with g the constant of gravity and $\underline{\underline{I}}$ is the 2×2 identity matrix.

In Section 2, we derive a different formulation of the shallow water equations that indicates the possible decomposition. Error analysis shows that this system can be approximated to any order of accuracy by a number of linear advection equations in conservative form which can be solved independently. The idea of transport can also be applied to this type of equations. The extension to a high order scheme follows in a natural way as shown in Section 3. We discuss a new idea for the limiting process and present a high order resolution scheme for the shallow water equations. In Section 4, we present numerical results obtained with the developed scheme for free surface flow problem.

2. Decomposition of the equations

In [2] and [5], the contributions are decomposed into two waves, $\underline{\mathcal{C}}^+$ and $\underline{\mathcal{C}}^-$. These waves are related to critical waves. It is the aim of this section to decompose the shallow water equations in a similar fashion. In [4] the decomposition is done for the Euler equations.

2.1. Decomposition in infinitely many advection equations.

Using the coefficients $\underline{R}_1$ and $\underline{\underline{L}}$ defined in [5] as,

$$\underline{R}_1 = h\begin{pmatrix} 1 \\ \underline{u} \end{pmatrix} \quad \text{and} \quad \underline{\underline{L}} = \frac{h\,c}{2}\begin{pmatrix} \underline{0}^T \\ \underline{\underline{I}} \end{pmatrix},$$

$\underline{\underline{\mathcal{F}}}$ can be written as

$$\underline{\underline{\mathcal{F}}}(\underline{U}) = \underline{R}_1\,\underline{u}^T + c\,\underline{\underline{L}}.$$

The propagation of the quantity $\underline{R}_1$ with the velocity $\underline{u}+c\,\underline{n}$ is a translation by $\underline{u}$ combined with an expansion $c\,\underline{n}$. For each $\underline{n}$ we can interpret the behaviour of $\underline{R}_1$ as a transport process described by

$$\underline{\phi}_1(\underline{n}) := (\underline{R}_1)_t + \nabla \cdot (\underline{R}_1(\underline{u} + c\,\underline{n})^T).$$

Since the critical waves move in all directions, we have to split $\underline{R}_1$ and propagate it in all directions. With the identities

$$\frac{1}{|S|}\int_S dS = 1 \quad \text{and} \quad \frac{1}{|S|}\int_S \underline{n}\, dS = 0,$$

where S is the unit sphere in $\mathbb{R}^N$, N is the space dimension in our case 2 and $|S|$ its surface. With the state vector $\underline{U}$ written as

$$\underline{U} = \frac{1}{|S|}\int_S \underline{R}_1\, dS,$$

the integral of $\underline{\phi}_1(\underline{n})$ over the unit sphere becomes

$$\frac{1}{|S|}\int_S \underline{\phi}_1(\underline{n})\, dS = \underline{U}_t + \nabla \cdot (\underline{U}\,\underline{u}^T).$$

However, this is not the left-hand side of the shallow water equations. The missing term in the flux matrix can be associated with the $\underline{\mathcal{C}}^-$ wave. The vector $\underline{\underline{L}}\,\underline{n}$ is also transported with the velocity $\underline{u}+c\,\underline{n}$. The corresponding transport terms are

$$\underline{\phi}_2(\underline{n}) := (\underline{\underline{L}}\,\underline{n})_t + \nabla \cdot (\underline{\underline{L}}\,\underline{n}(\underline{u} + c\underline{n})^T).$$

Clearly, since $\underline{\underline{L}}$ is independent of $\underline{n}$

$$\frac{1}{|S|}\int_S \underline{\underline{L}}\,\underline{n}\, dS = 0 \quad \text{and} \quad \frac{1}{|S|}\int_S \underline{n}\,\underline{n}^T\, dS = \frac{1}{N}\,\underline{\underline{I}}.$$

To get consistency with the shallow water equations (1), we take N times $\underline{\phi}_2$. Then the equations

$$\frac{1}{|S|}\int_S \underline{\phi}_a(\underline{n})\, dS = \underline{U}_t + \nabla \cdot \underline{\underline{\mathcal{F}}} = 0, \tag{2}$$

with

$$\underline{\phi}_a(\underline{n}) := \underline{\phi}_1(\underline{n}) + N\underline{\phi}_2(\underline{n})$$

recover the original nonlinear system. $\underline{\phi}_a(\underline{n})$ is the combination of the $\underline{\mathcal{C}}^+$ and $\underline{\mathcal{C}}^-$ waves. Using

$$\underline{R}_a(\underline{n}) := \underline{R}_1 + N\,\underline{\underline{L}}\,\underline{n},$$

we get for $\underline{\phi}_a$

$$\underline{\phi}_a(\underline{n}) = (\underline{R}_a)_t + \nabla \cdot (\underline{R}_a(\underline{u} + c\,\underline{n})^T).$$

Hence the state vector is represented by

$$\underline{U} = \frac{1}{|S|} \int_S \underline{R}_a(\underline{n})\, dS. \tag{3}$$

In the next section we shall make use of this representation to create a numerical scheme. The similar decomposition for the Euler equations is described in [4].

2.2. **Decomposition in finitely many advection equations.** The disadvantages of the formulations (2) and (3) are that the state vector $\underline{U}$ is represented by an integral and infinitely many advection equations have to be solved. The integral will now be replaced by a finite sum of k terms. (3) becomes

$$\underline{U} = \frac{1}{k} \sum_{i=1}^{k} \underline{R}_a(\underline{n}_i) = \frac{1}{k} \sum_{i=1}^{k} \left(\underline{R}_1 + N\, \underline{\underline{L}}\, \underline{n}_i \right) \tag{4}$$

and (2)

$$\frac{1}{k} \sum_{i=1}^{k} \underline{\phi}_a(\underline{n}_i) = \underline{U}_t + \nabla \cdot \underline{\underline{\mathcal{F}}} = 0. \tag{5}$$

In order that (4) and (5) hold exactly, the $\underline{n}_i$ have to satisfy certain conditions. From equation (4) follows

$$\sum_{i=1}^{k} \underline{n}_i = 0 \tag{6}$$

and from (5)

$$\frac{N}{k} \sum_{i=1}^{k} \underline{n}_i\, \underline{n}_i{}^T = \underline{\underline{I}}. \tag{7}$$

Collecting these results we can represent the shallow water equations (5) by a combination of k advection equations if (6) and (7) hold.
The condition (6) and (7) do not define $\underline{n}_i$ uniquely. Here we consider in particular the four vectors aligned on the horizontal and vertical axis, which are

$$\underline{n}_i \in \left\{ \begin{pmatrix} 1 \\ 0 \end{pmatrix}, \begin{pmatrix} 0 \\ 1 \end{pmatrix}, \begin{pmatrix} -1 \\ 0 \end{pmatrix}, \begin{pmatrix} 0 \\ -1 \end{pmatrix} \right\} \tag{8}$$

for $i = 1, \ldots, 4$. Note that this choice of $\underline{n}_i$ is not related to the dimensional splitting approach. In general the final propagations $\underline{u}+c\underline{n}_i$ are not aligned with the coordinate axes. These $\underline{n}_i$ are also a natural way to approximate the characteristic cone. The vectors $\underline{n}_i$ can be

interpreted as the support points for a quadrature rule to integrate the characteristic cone.
Another possible choice is given by the unit vectors lying on the diagonal. In this case strips along the edges of the exact support are not recovered. We solved this problem by replacing the vectors $\underline{n}_i$ by the $\widetilde{\underline{n}}_i$

$$\widetilde{\underline{n}}_i \in \left\{ \begin{pmatrix} 1 \\ 1 \end{pmatrix}, \begin{pmatrix} 1 \\ -1 \end{pmatrix}, \begin{pmatrix} -1 \\ 1 \end{pmatrix}, \begin{pmatrix} -1 \\ -1 \end{pmatrix} \right\} \tag{9}$$

for $i = 1, \ldots, 4$. The choice of $\widetilde{\underline{n}}_i$ is identical to the Method of Transport simple. To allow non unit vectors for the directions $\underline{n}_i$, we have to use a more general definition for $\underline{R}_a$.
We already introduced the scaling factor N to get consistency in (7). If we define $\underline{R}_a$ as

$$\widetilde{\underline{R}}_a(\widetilde{\underline{n}}_i) := \underline{R}_1 + \omega_i \, \underline{\underline{L}} \, \widetilde{\underline{n}}_i,$$

where

$$\omega_i := \frac{N}{\widetilde{\underline{n}}_i^T \widetilde{\underline{n}}_i},$$

we get exactly the shallow water equations

$$\frac{1}{k} \sum_{i=1}^{k} \widetilde{\underline{\phi}}_a(\widetilde{\underline{n}}_i) = \underline{U}_t + \nabla \cdot \underline{\underline{\mathcal{F}}} = 0, \tag{10}$$

$\underline{\phi}_a$ becomes

$$\widetilde{\underline{\phi}}_a(\widetilde{\underline{n}}_i) := (\widetilde{\underline{R}}_a(\widetilde{\underline{n}}_i))_t + \nabla \cdot (\widetilde{\underline{R}}_a(\widetilde{\underline{n}}_i) \, (\underline{u} + c \, \widetilde{\underline{n}}_i)^T). \tag{11}$$

Note, that even though the numerical celerity seem to be larger by a factor of $\sqrt{N}$ the CFL condition is not affected by this choices, i.e.

$$\Delta t \leq \min\left(\frac{\Delta x}{|u| + c}, \frac{\Delta y}{|v| + c}\right).$$

2.3. **High order corrections.** To solve the equations (10) for one timestep, we linearize $\widetilde{\underline{\phi}}_a(\widetilde{\underline{n}}_i)$ and set each component of the sum to zero. At a given time, t_0, we eliminate the time dependency of $\underline{u}$ and c by freezing the time so that

$$\underline{a}(\underline{x}, \widetilde{\underline{n}}_i) := \underline{u}(\underline{U}(\underline{x}, t_0)) + \widetilde{\underline{n}}_i \, c(\underline{U}(\underline{x}, t_0))$$

becomes a function of $\underline{x}$ only. Thus, we obtain a set of linear advection equations of the form

$$\widetilde{\underline{\phi}}_a(\widetilde{\underline{n}}_i) := (\widetilde{\underline{R}}_a(\widetilde{\underline{n}}_i))_t + \nabla \cdot (\widetilde{\underline{R}}_a(\widetilde{\underline{n}}_i) \, \underline{a}(\underline{x}, \widetilde{\underline{n}}_i)^T) = 0, \tag{12}$$

which we have to solve for one timestep Δt with initial conditions

$$\widetilde{\underline{R}}_a(\widetilde{\underline{n}}_i) = \underline{R}_1(\underline{U}(\underline{x}, t_0)) + \omega_i \, \underline{\underline{L}}(\underline{U}(\underline{x}, t_0)) \, \widetilde{\underline{n}}_i. \tag{13}$$

Summing up the solutions of (12) for $i = 1, \ldots, k$ leads to an approximate solution of (10), i.e.

$$\underline{U}(\underline{x}, t_0 + \Delta t) \cong \frac{1}{k} \sum_{i=1}^{k} \widetilde{\underline{R}}_a(\widetilde{\underline{n}}_i)(\underline{x}, t_0 + \Delta t). \tag{14}$$

The time evolution of the exact solution can be approximated by the average of the solutions of the decomposed equations. For a general nonlinear system, this approximation is only of first order.
A more accurate approximation can be found by replacing (13) by

$$\widetilde{\underline{R}}_a(\widetilde{\underline{n}}_i) = \underline{R}_1 + \omega_i \, (\underline{\underline{L}} + \underline{\underline{K}}) \, \widetilde{\underline{n}}_i. \tag{15}$$

The correction matrix $\underline{\underline{K}}$

$$\underline{\underline{K}}(\underline{x}, t_0) = \begin{pmatrix} k_{11} & k_{12} \\ k_{21} & k_{22} \\ k_{31} & k_{32} \end{pmatrix},$$

can be chosen such that the error after one timestep is of third order. It is determined by an error analysis in [7]. The components of $\underline{\underline{K}}$ are given by

$$k_{11} = -\frac{\Delta t}{2\,c}((1 - \frac{3\,\omega}{2})\, h_x\, c^2 + h\, u\, u_x + h\, u_y\, v)$$

$$k_{12} = -\frac{\Delta t}{2\,c}(h\, u\, v_x + (1 - \frac{3\,\omega}{2})\, h_y\, c^2 + h\, v\, v_y)$$

$$k_{21} = -\frac{\Delta t}{2\,c}((\frac{5}{4} - \frac{3\,\omega}{2}) h_x\, c^2\, u + (\frac{1}{2} - \omega) h\, c^2\, u_x + h\, u^2\, u_x + \frac{1}{4} h_y\, c^2\, v + h\, u\, u_y\, v + \frac{1}{2} h\, c^2\, v_y)$$

$$k_{22} = -\frac{\Delta t}{2\,c}(h\, u^2\, v_x + (1 - \frac{3\,\omega}{2})\, h_y\, c^2\, u - \omega\, h\, c^2\, u_y + h\, u\, v\, v_y)$$

$$k_{31} = -\frac{\Delta t}{2\,c}((1 - \frac{3\,\omega}{2})\, h_x\, c^2\, v + h\, u\, u_x\, v - \omega\, h\, c^2\, v_x + h\, u_y\, v^2)$$

$$k_{32} = -\frac{\Delta t}{2\,c}(\frac{1}{4} h_x\, c^2\, u + \frac{1}{2} h\, c^2\, u_x + h\, u\, v\, v_x + (\frac{5}{4} - \frac{3\,\omega}{2}) h_y\, c^2\, v + (\frac{1}{2} - \omega) h\, c^2\, v_y + h\, v^2\, v_y),$$

where

$$\omega = \frac{1}{k} \sum_{i=1}^{k} \underline{n}_{i,1}^2 = \frac{1}{k} \sum_{i=1}^{k} \underline{n}_{i,2}^2.$$

(15) shows that the corrected equations have the same structure as before. This is true even for higher order corrections.

3. Higher order scheme

In the previous section, we introduced a second order decomposition of the shallow water equations in a set of linear advection equations with variable coefficients. Now we want to present a high order numerical scheme to solve these linear equations. Therefore, we consider the two-dimensional advection equation in conservative form

$$u_t + \nabla \cdot (u\,\underline{a}^T) = 0, \tag{16}$$

with $\underline{a} = \underline{a}(\underline{x}) = (a, b)^T$. The advection equation (16) can be written as

$$u_t + (\nabla u) \cdot \underline{a} = -u\,(\nabla \cdot \underline{a}^T). \tag{17}$$

3.1. **Two-dimensional approach.** We want to extend the multidimensional Method of Transport to higher order. The Method of Transport is a finite volume method, where the update to the new timestep is done by adding incoming and subtracting outgoing flows with all the neighbouring cells. The final scheme in conservation form for the scalar equation reads

$$u_{\Omega_i}^{n+1} = u_{\Omega_i}^{n} - \frac{1}{|\Omega_i|} \sum_{j \neq i} (F_{\Omega_i \Omega_j} - F_{\Omega_j \Omega_i}),$$

where $|\Omega_i|$ is the area of the cell. The contributions $\underline{F}_{\Omega_i \Omega_j}$ represent the quantity of information which flows from domain Ω_i into domain Ω_j. The contributions $\underline{F}_{\Omega_i \Omega_j}$ approximate the physical multidimensional flux $\underline{\underline{\mathcal{F}}}$ and are defined as

$$F_{\Omega_i \Omega_j} = \int_{\Omega_j} \mathcal{U}(\underline{x}, t_0 + \Delta t)\, d\underline{x}.$$

The wave $\mathcal{U}$ describes the transport of u from the computational cell Ω_i to any point $\underline{x}$ in space and is given by

$$\mathcal{U}(\underline{x}, t_0 + \Delta t) = \int_{\Omega_i} u(\underline{\xi}, t_0) \delta(\underline{z}(t_0 + \Delta t, \underline{\xi}) - \underline{x})\, d\underline{\xi}. \tag{18}$$

δ is the Dirac's delta distribution and $\underline{z}(t_0 + \Delta t, \underline{\xi})$ is the characteristic curve along which the evolution of u in (17) satisfies

$$\frac{d}{dt} u(\underline{z}(t), t) = -u\,(\nabla \cdot \underline{a}^T).$$

The characteristic curve $\underline{z}(\tau)$ is defined as the solution of

$$\dot{\underline{z}}(\tau) = \underline{a}(\underline{z}(\tau)), \quad \underline{z}(t_0) = \underline{\xi}. \tag{19}$$

The integration of the delta distribution in (18) is not trivial, due to the nonlinear argument. Assuming the map defined in (19) to be bijective, then the variable transformation

$$\underline{v}(\underline{\xi}, \underline{x}) := \underline{z}(t_0 + \Delta t, \underline{\xi}) - \underline{x}$$

has an inverse $\underline{s}(\underline{v}, \underline{x})$, i.e. $\underline{v} \circ \underline{s} = Id$, which allows the integration of the delta function. Thus, the computation of the contributions $F_{\Omega_i\Omega_j}$ becomes

$$F_{\Omega_i\Omega_j} = \int_{\Omega_j} u(\underline{s}(0, \underline{x}), t_0) \, \frac{1}{\det(J)} \, d\underline{x}, \tag{20}$$

where $J = d\underline{z}/d\underline{\xi}$ is the Jacobian of the mapping in (19).
It turns out, that the integration of (19) determines the accuracy in time, where as the reconstruction of the function u in cell Ω_i limits the spatial accuracy. For this reason, choosing constant values for a and u in each cell leads to first order scheme. In this case, the wave $\mathcal{U}$ is given by

$$\mathcal{U}(\underline{x}, t_0 + \Delta t) = \int_{\Omega_i} u(\underline{\xi}, t_0) \delta(\underline{x} - \Delta t \, \underline{a} - \underline{\xi}) \, d\underline{\xi}$$

and the contributions by

$$F_{\Omega_i\Omega_j} = \int_{\Omega_j} u(\underline{x} - \Delta t \, \underline{a}, t_0) \, d\underline{x}.$$

To get a second order approximation of the characteristic curve we take a linear reconstruction for $\underline{a}(\underline{z})$

$$\underline{a}(\underline{z}) = \underline{a} + \underline{\underline{A}} \, \underline{z}, \tag{21}$$

where the matrix $\underline{\underline{A}}$ is defined as

$$\underline{\underline{A}} = \begin{pmatrix} a_x & a_y \\ b_x & b_y \end{pmatrix}.$$

Since $\underline{\underline{A}}$ is constant, the solution of the corresponding linear differential equation

$$\dot{\underline{z}}(\tau) = \underline{a} + \underline{\underline{A}} \, \underline{z}, \quad \underline{z}(t_0) = \underline{\xi}$$

is given by

$$\underline{z}(\tau) = -\underline{\underline{A}}^{-1} \, \underline{a} + e^{\underline{\underline{A}}\tau} (\underline{\underline{A}}^{-1} \, \underline{a} + \underline{\xi}).$$

Taking the Taylor expansion of $\underline{z}(\tau)$

$$\underline{z}(\tau) = \underline{\xi} + \tau \, (\underline{a} + \underline{\underline{A}} \, \underline{\xi}) + \frac{\tau^2}{2} (\underline{\underline{A}} \, \underline{a} + \underline{\underline{A}}^2 \, \underline{\xi}) + O(\tau^3),$$

we get

$$\underline{z}(t_0+\Delta t,\underline{\xi}) = \underline{\xi} + \Delta t\,(\underline{a} + \underline{\underline{A}}\,\underline{\xi}) + \frac{\Delta t^2}{2}(\underline{\underline{A}}\,\underline{a} + \underline{\underline{A}}^2\,\underline{\xi}) + O(\Delta t^3). \tag{22}$$

Substituting (22) into $\underline{v}(\underline{\xi},\underline{x})$, the equations

$$\underline{v}(\underline{\xi},\underline{x}) = 0$$

can be solved and the solution is

$$\underline{s}(\underline{0},\underline{x}) = (\underline{\underline{I}} + \Delta t\,\underline{\underline{A}} + \frac{\Delta t^2}{2}\underline{\underline{A}}^2)^{-1}(\underline{x} - \Delta t\,\underline{a} - \frac{\Delta t^2}{2}\underline{\underline{A}}\,\underline{a}) + O(\Delta t^3).$$

Using the Neumann series we get as second order approximation

$$\begin{aligned}\underline{s}(\underline{0},\underline{x}) &= (\underline{\underline{I}} - \Delta t\,\underline{\underline{A}} + \frac{\Delta t^2}{2}\underline{\underline{A}}^2)(\underline{x} - \Delta t\,\underline{a} - \frac{\Delta t^2}{2}\underline{\underline{A}}\,\underline{a}) + O(\Delta t^3)\\ &= \underline{x} - \Delta t\,\underline{\underline{A}}\,\underline{x} - \Delta t\,\underline{a} + \frac{\Delta t^2}{2}\underline{\underline{A}}\,\underline{a} + \frac{\Delta t^2}{2}\underline{\underline{A}}^2\underline{x} + O(\Delta t^3).\end{aligned}$$

By the variable substitution $\underline{x} = \underline{s}(0,\underline{y})$ we get for the contributions

$$F_{\Omega_i\Omega_j} = \int_{\underline{s}(0,G_j)} u(\underline{x},t_0)\,d\underline{x},$$

where $\underline{s}(0,G_j) \subset \Omega_i$ describes the inverse of the domain G_j, which is sketched in Figure 1.
The domains of integration can be triangles, quadrilaterals, pentagons or hexagons. To get second order in space, we reconstruct $u(x)$ linearly and use a quadrature rule to get the contributions.
We can check that with the contributions $F_{\Omega_i\Omega_j}$ defined above, the numerical method is of second order. Further explanation about the scheme can be found in [3] and [4].

3.2. **Limiting process.** In this subsection we study two limiting processes for conservation laws. They are based on first order solutions which we assume to converge to the physically correct solutions. We discuss two type of limiters, namely the slope-limiter and the contribution-limiter method. For stability reasons, all second order methods must degenerate to first order near discontinuities. Unfortunately, this also causes a degeneration near extreme points. Only a very few limiter functions overcome this problem [8].
For simplification, we consider the contributions $\underline{F}_{\Omega_i\Omega_j}$ for the one dimensional case. For the first order scheme we get

$$F_{\Omega_i\Omega_{i+1}} = \begin{cases} \Delta t\,a_i\,u_i & \text{if} \quad a_i > 0 \\ 0 & \text{else} \end{cases}.$$

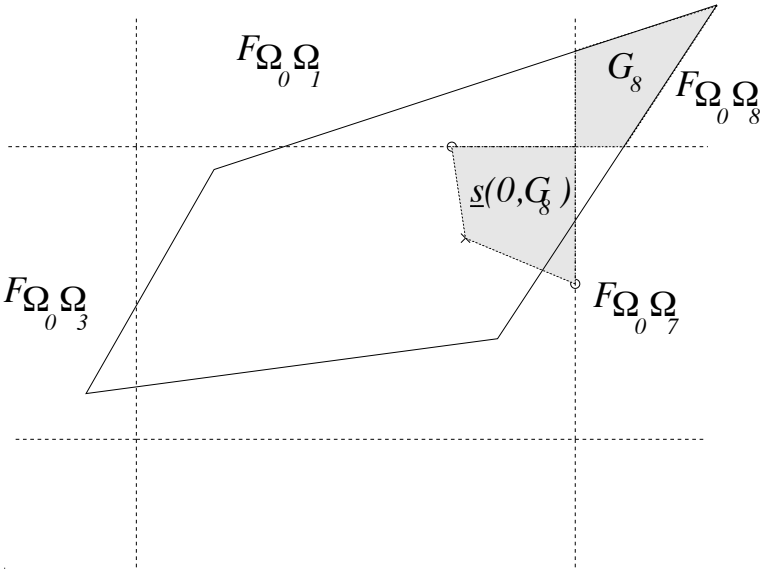

FIGURE 1. Sketch of transformation (28). The solid line represents the forward transformation of the original cell. The dotted line denotes the backward transformation of G_8 into the original cell.

With the notation of section 3.1, the second order scheme reads

$$F_{\Omega_i\Omega_{i+1}} = \int_{s(0,x_{i+1/2})}^{x_{i+1/2}} (u_i + (u_x)_i\, x)\, dx,$$

where

$$s(0, x_{i+1/2}) = s(0, x_i + \frac{\Delta x}{2}) = \frac{\Delta x}{2} - \Delta t\, a - \Delta t\, a_x\, \frac{\Delta x}{2} + \frac{\Delta t^2}{2}\, a\, a_x.$$

This is equivalent to

$$F_{\Omega_i\Omega_{i+1}} = \Delta t[a_i\, u_i + (1 - \frac{\Delta t}{\Delta x}\, a)\, ((a_x)_i\, u_i + a_i\, (u_x)_i)\frac{\Delta x}{2}],$$

if $s(0, x_{i+1/2}) < x_{i+1/2}$. The x-derivatives of a and u can be approximated in different ways. First order approximation is sufficient to get a second order scheme, if the same stencil is used everywhere. Unfortunately, limiter functions will switch between different stencils even in smooth regions, e.g. extreme or saddle points. To keep second order accuracy it is sufficient to use the first derivatives but with a better

approximation than $O(\Delta x)$ like

$$
\begin{aligned}
(u_x)_i^{upwind} &= \frac{-u_{i+2} + 4\,u_{i+1} - 3\,u_i}{2\,\Delta x}, \\
(u_x)_i^{central} &= \frac{u_{i+1} - u_{i-1}}{2\,\Delta x}, \\
(u_x)_i^{downwind} &= \frac{3\,u_i - 4\,u_{i-1} + u_{i-2}}{2\,\Delta x}.
\end{aligned} \tag{23}
$$

The first limiting strategy uses a slope-limiter. The slope in cell Ω_i is given by one of these three different finite differences

$$
(u_x)_i = \begin{cases}
(u_x)_i^{upwind} & \text{if } |(u_x)_i^{upwind}| = \min_3 \\
(u_x)_i^{central} & \text{if } |(u_x)_i^{central}| = \min_3 \\
(u_x)_i^{downwind} & \text{if } |(u_x)_i^{downwind}| = \min_3
\end{cases} \tag{24}
$$

where $\min_3 = \min(|(u_x)_i^{upwind}|\,,\, |(u_x)_i^{central}|\,,\, |(u_x)_i^{downwind}|)$.
The scheme with this limiter is essentially non oscillatory for the advection equation. For the shallow water equations, this limiter does not prevent overshoots and oscillations at discontinuities. This phenomena is also observed with all sort of slope-limiters, e.g. the minmod, van Leer, superbee limiters.
This ENO-like strategy gets worse in several space dimensions since the numbers of possible stencils increases drastically, e.g. 33 in the two-dimensional case compared to the three in (23). In addition to this, the limiting process introduces a new grid dependence, since grid aligned gradients are treated differently than oblique ones.
The second strategy uses a contribution-limiter and is based on the non oscillatory character of the first order solution. To conserve this property, we compute the first and second order solution without any limiter. The derivatives in the high order computation are always approximated by the central difference. The next timestep is then given by

$$
u_{\Omega_i}^{n+1} = u_{\Omega_i}^{n} - \frac{1}{|\Omega_i|} \sum_{j \in V} \Delta\, F_{\Omega_i \Omega_j},
$$

where $\Delta\, F_{\Omega_i \Omega_j} = F_{\Omega_i \Omega_j} - F_{\Omega_j \Omega_i}$. We want to use the second order contributions if

$$
\min_{j \in V} (u_j^{n+1})^1 \le (u_i^{n+1})^2 \le \max_{j \in V} (u_j^{n+1})^1, \tag{25}
$$

where $V = \{i-1, i, i+1\}$, otherwise the first order contributions are taken. The superscripts 1 and 2 denotes the order of the quantities between brackets. To keep the method conservative, $F_{\Omega_i \Omega_j}$ has to be chosen more restrictive. If the cell Ω_i or Ω_j is marked to be of first

order, then $F_{\Omega_i\Omega_j}$ includes the first order contributions from both sides, otherwise the second order terms are used. In addition if

$$(\Delta F_{\Omega_i\Omega_j})^1 \cdot (\Delta F_{\Omega_i\Omega_j})^2 \leq 0$$

the first order contribution has to be chosen.
For the one-dimensional advection and shallow water equations, this limiter performs very well. The speed of the discontinuity or the shock is correct resolved. The same idea can naturally be extend to the two-dimensional case. The decision, which contribution to take, is related to the results of two multidimensional methods and is independent of the grid as the methods. In (25) the indices i and j become multi-indices $i = (i_1, i_2)$ and $j = (j_1, j_2)$. The set of all neighbours is $V = \{(i_1 + k, i_2 + l); l, k \in \{-1, 0, 1\}$.
For the shallow water equations this limiter prevents overshoots and oscillations at discontinuities.

4. Numerical results

This method is implemented on a parallel machine, with domain decomposition strategy. It performs very well on the Intel paragon. We have simulated different problems such as the abrupt expansion in a channel or the explosion problem. A more delicate one is the shock focusing problem. The results show the advantage of the multidimensional method compared with a dimension splitting scheme.

4.1. **Shock Focusing Problem.** Solving a rotational symmetric problem on a Cartesian mesh causes a lot of problems for any kind of numerical method. In the case of the shallow water equations, we compute the circular shock focusing problem as defined in [1]. The initial values are given by

$$g \cdot h(\underline{x}, 0) = \begin{cases} 0.1 & \text{if } |\underline{x}| \leq 0.35 \\ 1 & \text{else} \end{cases}$$

and $\underline{u}(\underline{x}, 0) = 0$. The two-dimensional calculations are done on the square domain $[-1.5, 1.5]^2$ with 160 points in each direction and $\Delta t = 0.008$, which corresponds to a CFL number of 1. Results are shown at time $t = 1.0$.
At time $t = 0$, a circular shock of the initial discontinuity moves inwards. At time $t = 1.0$, the initial circular shock has passed through the singularity and a circular shock is expanding outward from the centre and is interacting with the rarefaction wave.
Figure 2 shows the geopotential and the total velocity along cuts of $y = 0$ and $x+y = 0$ of the first order solution and the radial symmetrical

solution with 10000 points, which is a good approximation of the exact solution.
Figure 3 shows the second order solution, computed with the slope limiter (24). For the total velocity we observe a large difference between the two strips at time $t = 1$. This difference results from errors produced at the focusing point. Until the shock reaches the focusing point, the symmetry is preserved. For this limiter the difference between the two cuts does not converge to zero when the mesh size tends to zero.
This effect can be observed in [1], where the solution is computed with a operator split scheme using a van Leer limiter. It also appears in the solution computed with the software package CLAWPACK. A second order Godunov method described in [6] is used with a minmod limiter (see Figure 4). Furthermore the first order solution from CLAWPACK presents a difference between the x and the diagonal strip.
In a first approach to solve this problem we increased the number of propagation directions $\underline{n}_i$ up to 32 satisfying (6) and (7), but the difference did not decrease essentially.
We noticed that the second order solution without limiter function, i.e. using always the central difference to compute the slopes, does not present this problem (see Figure 5). This indicates that the loss of symmetry is due to the limiter.
The use of the contribution-limiter (25) removes this behaviour (see Figure 6). We observe that the structure of the x and the diagonal strips are almost identical and the solution converges for step size to zero.

Acknowledgments

The project at SAM is partly funded by the Ercoftac fellowship program. The authors would like to thank both Prof. R. Jeltsch his constant support.

References

[1] S. J. Billett, *A Class of Upwind Methods for Conservation Laws*, PhD thesis, Cranfield University, 1994.
[2] M. Fey, *Ein echt mehrdimensionales Verfahren zur Lösung der Eulergleichungen*, PhD thesis, ETH Zürich, 1993.
[3] ———, *Decomposition of the multidimensional euler equations into advection equations*, Tech. Report 95-14, Seminar für Angewandte Mathematik, ETH Zürich, 1995.
[4] M. Fey, R. Jeltsch, and A.-T. Morel, *Multidimensional schemes for nonlinear systems of hyperbolic conservation laws*, in Numerical Analysis 1995, D. Griffiths and G. Watson, eds., Longman, 1996.

[5] M. Fey and A.-T. Morel, *Multidimensional method of transport for the shallow water equations*, Tech. Report 95-05, Seminar für Angewandte Mathematik, ETH Zürich, 1995.

[6] R. LeVeque, *Simplified multi-dimensional flux limiter methods*, in Numerical Methods for Fluid Dynamics 4, M. Baines and K. Morton, eds., Oxford University Press, 1993.

[7] A.-T. Morel, *Multidimensional scheme for the shallow water equations*, in Proceedings of the Hydroinformatics 96 Conference, Zürich, 9-13 September 1996, A.A. Balkema Publishers, 1996.

[8] C. W. Schulz-Rinne, *The Riemann problem for the two-dimensional gas dynamics and new limiters for high-order schemes*, PhD thesis, ETH Zürich, 1993.

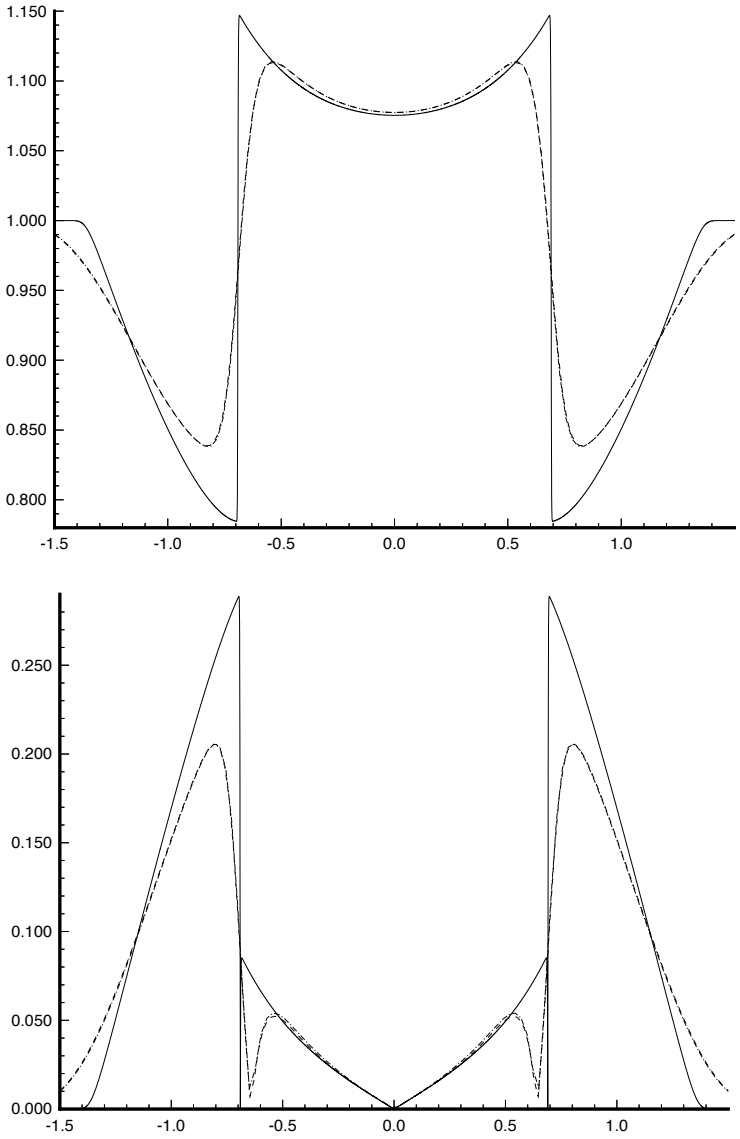

FIGURE 2. The dashed line represents the x-strip and the dashdotted line the diagonal strip from the first order scheme. The solid line represents the first order radial symmetric solution.

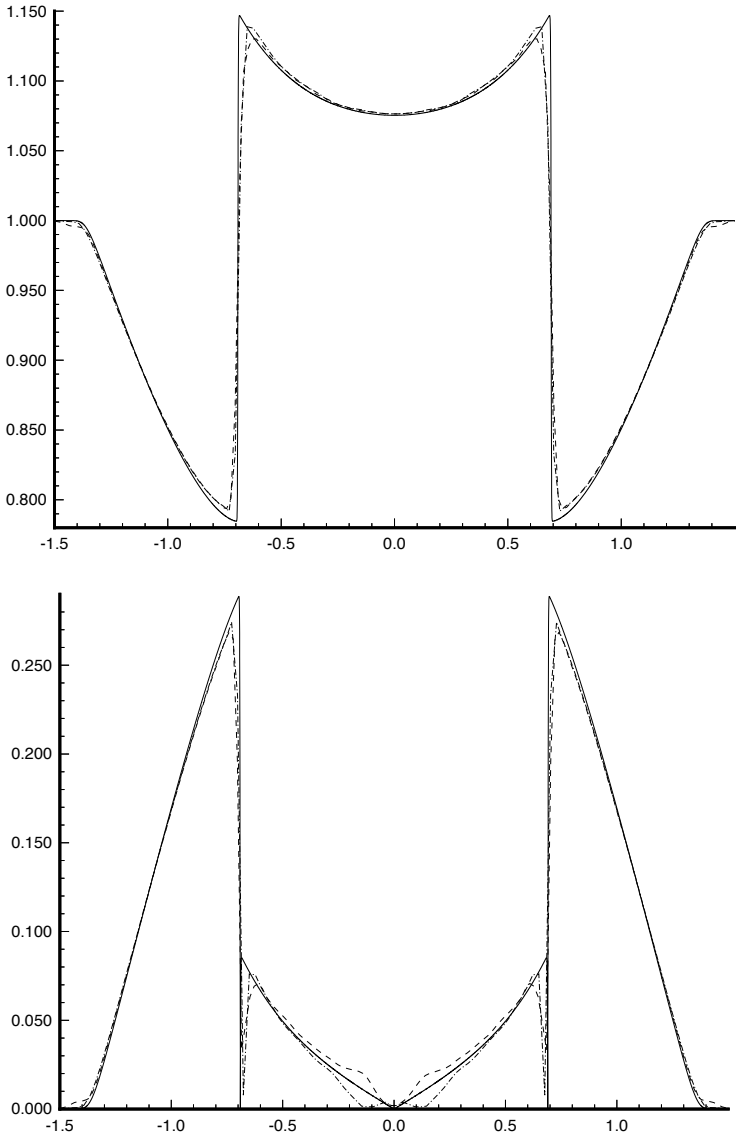

FIGURE 3. The dashed line represents the x-strip and the dashdotted line the diagonal strip from the second order scheme. The solid line represents the first order radial symmetric solution.

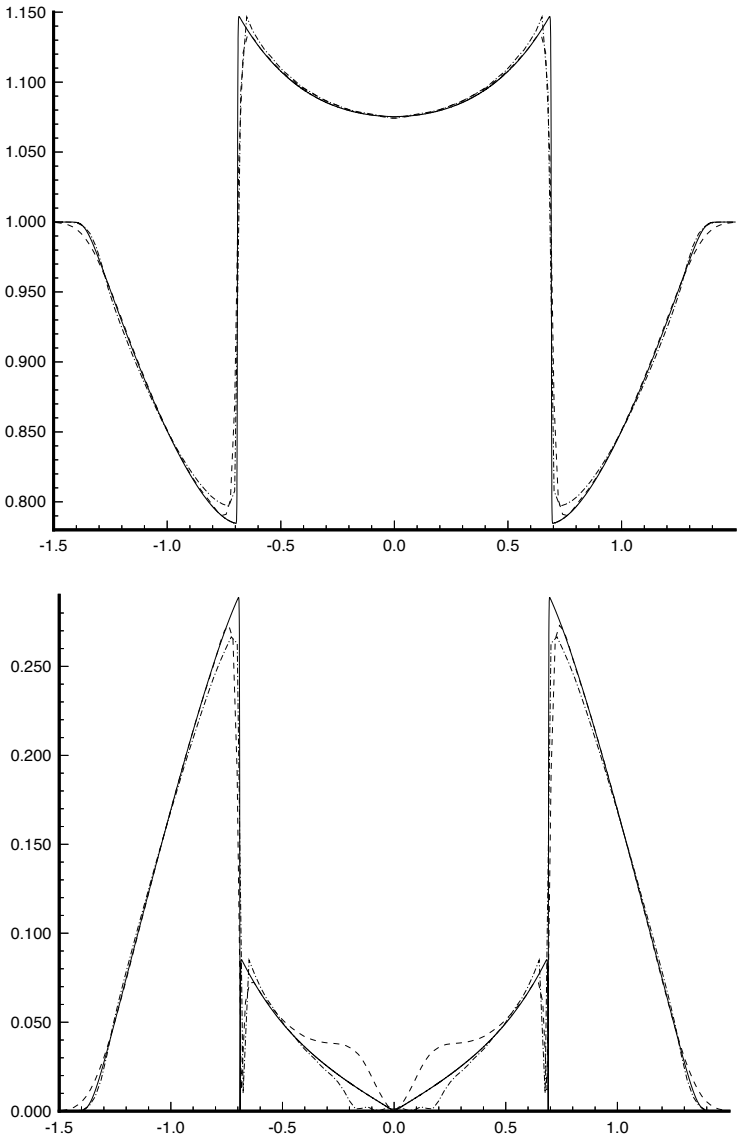

FIGURE 4. The dashed line represents the x-strip and the dashdotted line the diagonal strip from the second order scheme computed with the software package CLAWPACK. The solid line represents the first order radial symmetric solution.

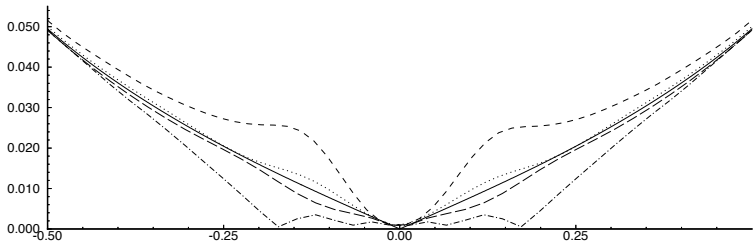

FIGURE 5. The dashed, dashdotted and solid lines are enlargements of the previous figure, the dotted and long-dashed lines represent the x and the diagonal strip from the second order solution computed without limiter.

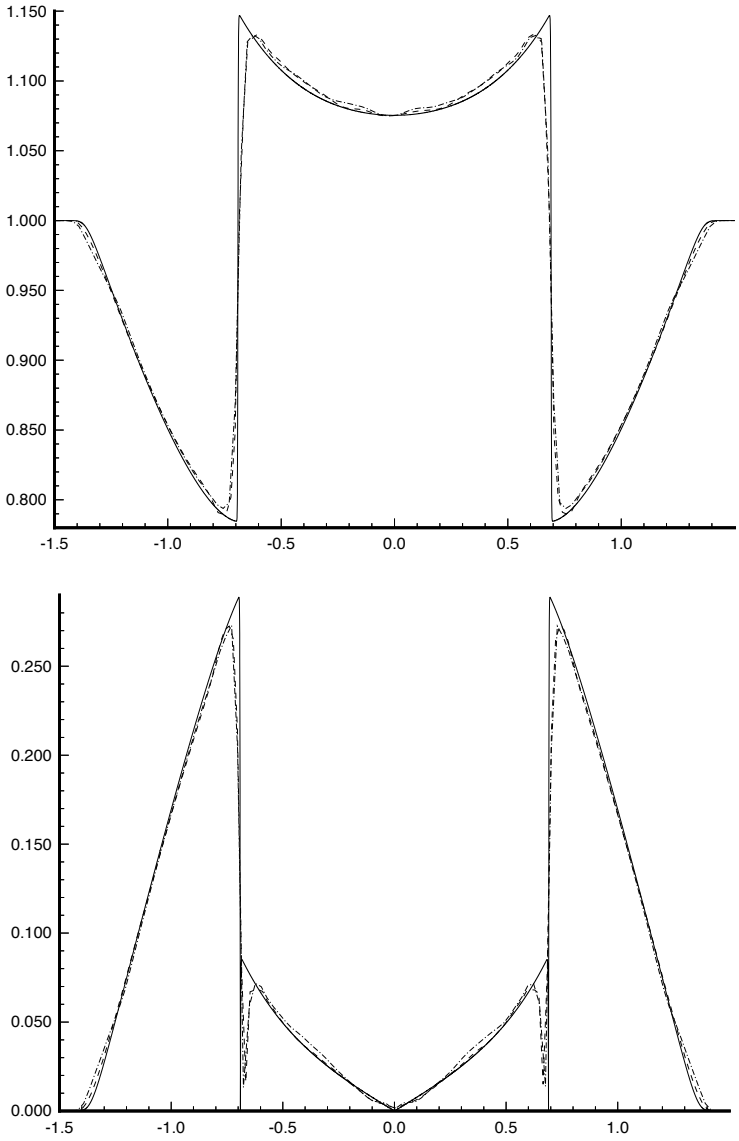

FIGURE 6. The dashed line represents the x-strip and the dashdotted line the diagonal strip from the second order scheme with the contribution-limiter. The solid line represents the first order radial symmetric solution.

Research Reports

No.	Authors	Title
96-09	A.-T. Morel, M. Fey, J. Maurer	Multidimensional High Order Method of Transport for the Shallow Water Equations
96-08	A.-T. Morel	Multidimensional Scheme for the Shallow Water Equations
96-07	M. Feistauer, C. Schwab	On coupled problems for viscous flow in exterior domains
96-06	J.M. Melenk	A note on robust exponential convergence of finite element methods for problems with boundary layers
96-05	R. Bodenmann, H.J. Schroll	Higher order discretisation of initial-boundary value problems for mixed systems
96-04	H. Forrer	Boundary Treatment for a Cartesian Grid Method
96-03	S. Hyvönen	Convergence of the Arnoldi Process when applied to the Picard-Lindelöf Iteration Operator
96-02	S.A. Sauter, C. Schwab	Quadrature for *hp*-Galerkin BEM in $\mathbb{R}^3$
96-01	J.M. Melenk, I. Babuška	The Partition of Unity Finite Element Method: Basic Theory and Applications
95-16	M.D. Buhmann, A. Pinkus	On a Recovery Problem
95-15	M. Fey	The Method of Transport for solving the Euler-equations
95-14	M. Fey	Decomposition of the multidimensional Euler equations into advection equations
95-13	M.D. Buhmann	Radial Functions on Compact Support
95-12	R. Jeltsch	Stability of time discretization, Hurwitz determinants and order stars
95-11	M. Fey, R. Jeltsch, A.-T. Morel	Multidimensional schemes for nonlinear systems of hyperbolic conservation laws
95-10	T. von Petersdorff, C. Schwab	Boundary Element Methods with Wavelets and Mesh Refinement
95-09	R. Sperb	Some complementary estimates in the Dead Core problem
95-08	T. von Petersdorff, C. Schwab	Fully discrete multiscale Galerkin BEM
95-07	R. Bodenmann	Summation by parts formula for noncentered finite differences
95-06	M.D. Buhmann	Neue und alte These über Wavelets
95-05	M. Fey, A.-T. Morel	Multidimensional method of transport for the shallow water equations